2.1 Introduction

Currently, one of the main research topics in condensed matter deals with the electronic properties of ultrathin compounds for which the scientific community has consecrated a significant effort since the discovery of graphene in 2004[1–3]. This young field experienced a big boost recently thanks to the isolation of atomically thin semiconductors based on transition metal dichalcogenides (TMD), such as MoS_2 and WSe_2. In contrast with graphene, these materials in their monolayer form are semiconductors with direct electronic bandgaps in the visible and near infrared range. The direct bandgap of monolayers and their efficient coupling with light makes them versatile and promising fundamental bricks for future nanoelectronics and optoelectronic devices [4–8]. Weak screening in 2D is also responsible for the formation of robust excitonic quasiparticles and the presence of strong many-body effects even at room temperature, making 2D TMDs ideal plattforms for fundamental studies in condensed matter. Moreover, their band structure is unique in the sense that the valley degree of freedom is strongly coupled with the spin, permitting the initialization and readout of the electron's valley/spin with polarized light. In this chapter, I introduce the fundamental properties of TMD monolayers before presenting a selection of my publications related to this topic.

2.2 Transition metal dichalcogenides: crystal symmetry and band structure

In their bulk form, TMDs are constituted of a stack of 2D layers (or monolayers) weakly coupled by van der Waals interactions, as shown in Fig.1(a). The hexagonal structural polytype, which is the most common for bulk TMDs, is the only one that will be considered here. Each monolayer is described by a triangular Bravais lattice consisting on a sheet of transition metal atoms M (M=Mo,W) sandwiched between two sheets of chalcogen atoms X (X=S,Se,Te). The weak van der Waals forces between layers make it possible to separate them in a variety of ways, for instance with the help of adhesive tape [9] (the so-called "mechanical exfoliation method") or by ion intercalation in a liquid solution [10]. Nowadays, monolayers can also be chemicaly grown directly onto a variety of substrates[11]. While bulk TMDs in the hexagonal phase are indirect bandgap semiconductors, reducing the material thickness eventually change the valley structure (*i.e.* the position of the conduction band minima and valence band maxima). In 2010, it was shown that monolayer MoS_2 has a direct bandgap at the K points of the hexagonal Brillouin zone [12,13], whereas bilayer (or thicker) MoS_2 remains an indirect bandgap semiconductor. Quantum confinement effects, which are stronger for the wavefunctions involved in the indirect transition*, are responsible for this change in the band structure, illustrated in Fig.1(b) which shows the results of Density Functional Theory[12] for MoS_2[2].

* The wavefunctions at the K valleys are mostly composed of transition metal d-orbitals, which are therefore not very sensitive to the number of layers.

A consequence of this change in band structure is the dramatic enhancement of the photoluminescence (PL) yield for monolayers, which are at least three orders of magnitude brighter than their bulk counterparts[14]. Figure 1(c) shows the measured PL spectrum of several TMD monolayers at room temperature.

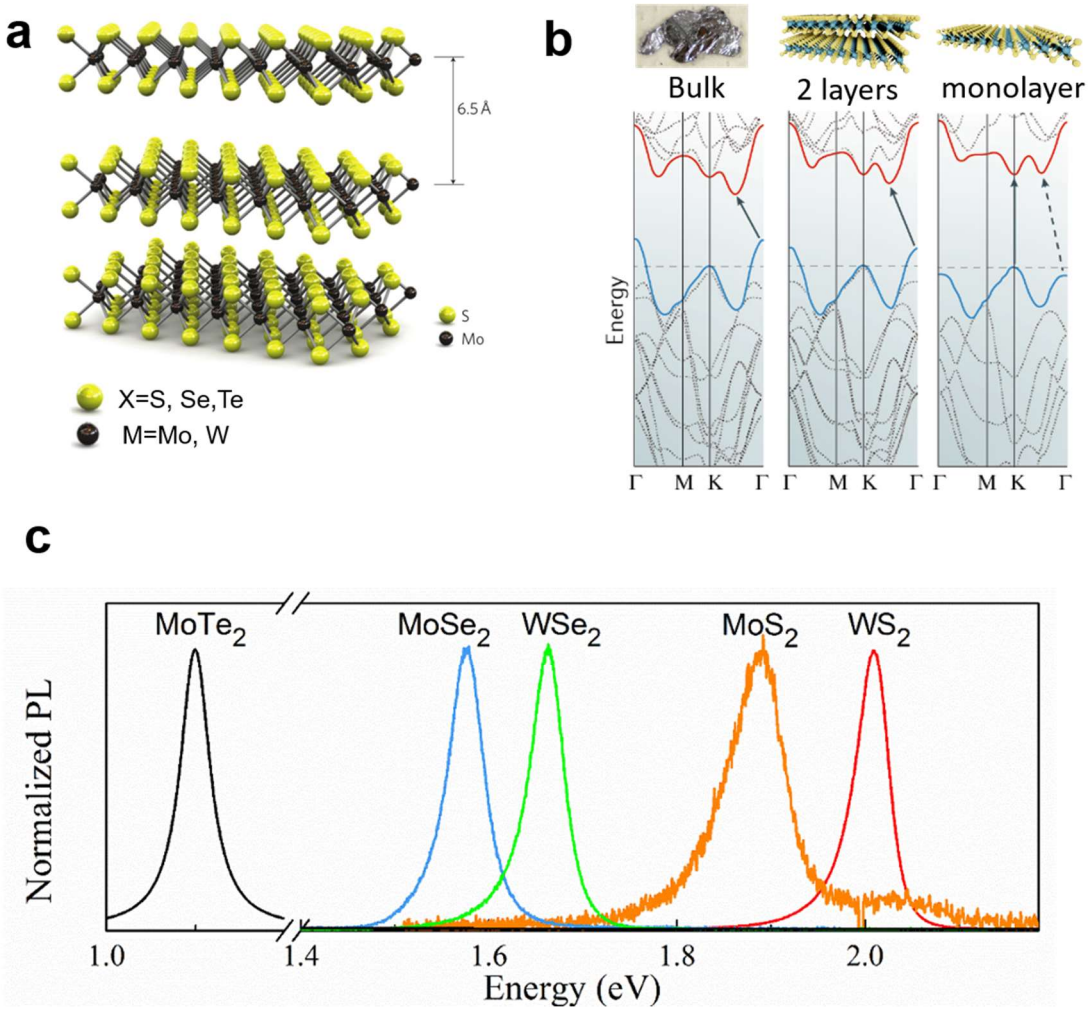

Figure 1: (a) Crystalline arrangement of MX_2 compounds, where M = W, Mo and X = S, Se, Te (from [4]). They are constituted of a stack of monolayers weakly coupled by van der Waals forces. (b) Calculated band structure of MoS_2 for different thicknesses. A direct bandgap occurs in the monolayer at the K points, whereas the bandgap is indirect for two or more layers. The solid arrows indicate the lowest energy transition between the valence band and the conduction band in each case, defining the bandgap. Modified from [12]. (c) Photoluminescence spectrum of different TMD monolayers at room temperature.

2.3 Spin-valley coupling

Most of the remarkable properties of TMDs are related to their electronic band structure in the 2D limit. The interplay between broken inversion symmetry and a strong spin-orbit interaction leads to a quite unique spin texture of the K^+ and K^- valleys (the two non-equivalent valleys located at the corners of the hexagonal Brillouin zone), precisely where the

bandgap is located at. Fig.2(a) shows the measured dispersion of the occupied states in monolayer $MoSe_2$ obtained by angular resolved photoemission spectroscopy (ARPES). It is observed that the valence band at the K valleys is splitted by hundreds of meV into two subbands due to the spin-orbit interaction, in agreement with DFT calculations[15]. The topmost valence subband is therefore spin-polarized, with a well-defined out-of-plane spin orientation which changes sign between the K^+ and the K^- valley due to time-reversal symmetry. This spin polarization of the valence subbands has been recently confirmed experimentally with spin-resolved ARPES on monolayer MoS_2 epitaxially grown on a gold surface [16], as shown in Fig.2(b). The spin-orbit interaction is also responsible for a splitting of the conduction band at the K valleys, although the splitting is typically one order of magnitude smaller than in the valence band, in the order of tens of meV [17].

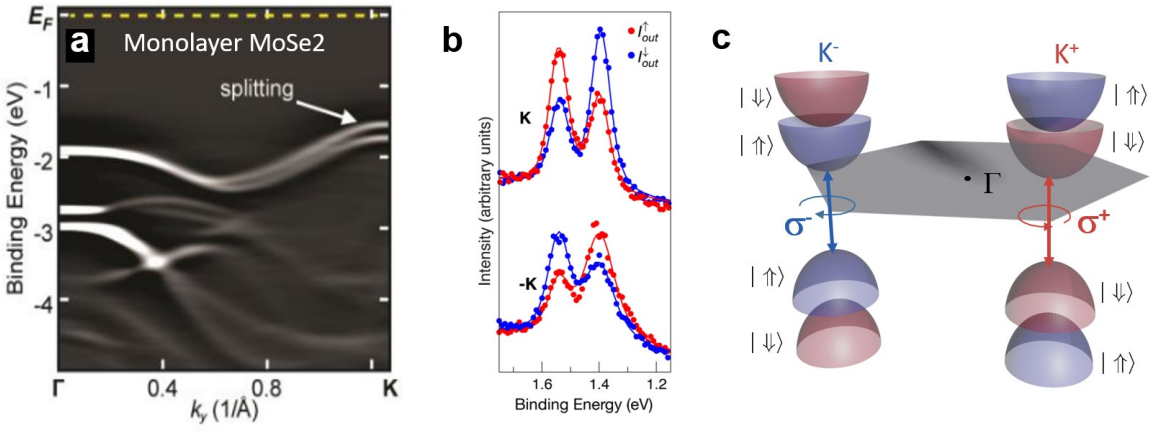

Figure 2: (a) ARPES spectrum of monolayer $MoSe_2$. From [18]. (b) Out-of-plane spin-resolved energy distribution curves at the K^+ and K^- points; with red and blue curves representing the up and down spins, respectively. From [16]. (c) Schematics of the band structure of a TMD monolayer near the K points. The electrons and holes lie on two kinds of non-equivalent valleys, K^+ and K^-, each one admitting only one possible spin state at a given energy, represented here by the arrows. The optical selection rules at these valleys permits to address the spin with circularly-polarized light, where σ^+ and σ^- represents the helicity of the circularly-polarized photons.

Due to these large spin-orbit splittings, in a given valley and at a fixed energy an electron can have only one possible spin state, in sharp contrast to what is found in traditional semiconductors. This is illustrated in Fig.2 (c). Thanks to this spin-valley coupling, the spin states are connected to optical transitions via chiral selection rules. In other words, one can simply initialize and detect the valley/spin DOF by using and detecting right – or left – circularly polarized light. These valley-selective optical selection rules do not exist in traditional semiconductors, and allow one to optically excite into a desired valley and/or to detect the state of the valley by measuring optical properties, opening the door for novel applications regarding information treatment [19–21]. Indeed, the spin/valley index for individual electrons (or holes) represents a very robust quantum state, since it is protected against inter-valley scattering. The reason is that for an electron to go from K^+ to K^-, for example, there needs to be a significant momentum change and a simultaneous spin-flip, making therefore

this process highly unlikely. Recently, in 2021, time-resolved magneto-optical experiments based on Kerr rotation have measured valley/spin lifetimes of resident carriers as long as tens of microseconds in doped WSe_2 monolayers at cryogenic temperatures[22], confirming the robustness of the vally index. However, the valley polarization measured in photoluminescence experiments decays in a much shorter timescale, in the picosecond range[23–25], due to strong excitonic effects which will be discussed below.

2.4 Tightly bound excitons in TMDs

As mentioned previously, circularly-polarized light can in principle be used to selectively populate a given valley with electrons and holes. However, light absorption in TMDs couples almost exclusively with bound electron-hole pairs (excitons) which are stable even at room temperature[26]. These excitons completely determine the optical properties such as absorption and PL. The robustness of excitons in TMDs is due to a combination of the following factors: i) confinement in 2D alone is responsible for 4-fold increase of the binding energy, ii) large effective masses for both electrons and holes, in the order of $m^* = 0.5\ m_e$ where m_e is the electron mass, and iii) weak dielectric screening due to the surrounding dielectric medium (typically air/vacuum, SiO_2 or hexagonal boron nitride). Excitons in TMDs have therefore unusually large binding energies of a few hundred meV [27,28], much larger than in traditional semiconductors.

As a consequence, a series of discrete resonances appear in the optical absorption spectrum at energies well below the free-particle bandgap, as illustrated in Fig.3(a). These discrete energy levels correspond to the different excitonic states, and are labelled according to an integer quantum number (n = 1, 2, 3, …) and orbital labels ($s,p,d,…$) in analogy with the Rydberg series of the hydrogen atom.

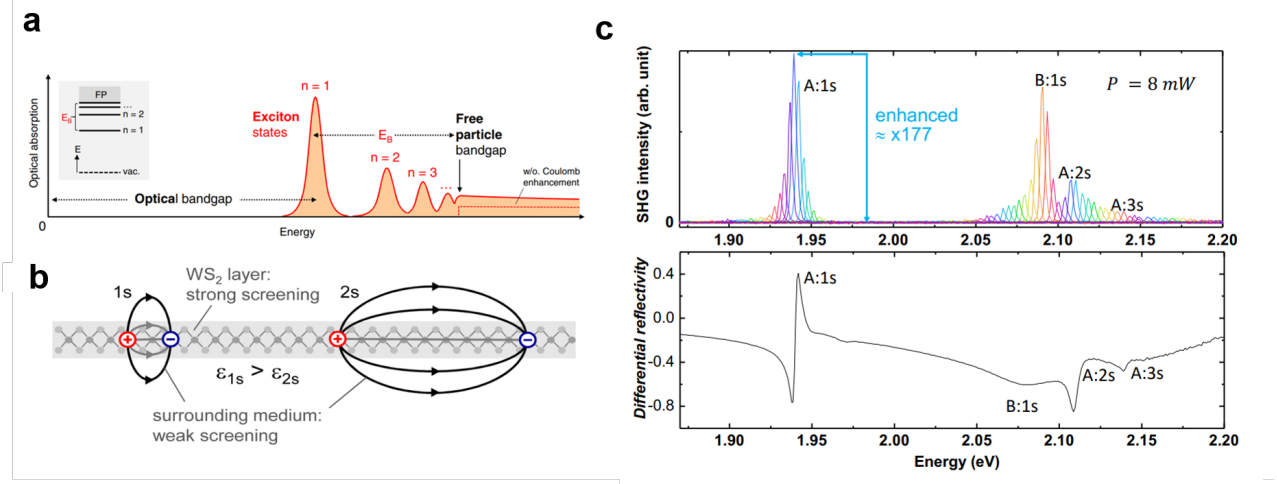

Figure 3: (a) Optical absorption spectrum of a TMD monolayer, exhibiting a series of resonances corresponding to the discrete excitonic levels within the bandgap, which are also illustrated in the inset. From [29]. (b) Schematic representation of eletron-hole pairs forming 1s and 2s states in a non-homogeneous dielectric environment. From [30]. (c) Comparison between SHG (top) and differential reflectivity spectra of monolayer MoS_2 (bottom). From [31].

The exciton ground state ($1s$) is therefore the lowest energy transition which dominates the absorption and defines the optical bandgap. The difference with respect to the free particle bandgap, which can be measured by Scanning tunneling spectroscopy (STS)[32], corresponds to the exciton binding energy.

A consequence of the 2D confinement is that the interaction strength between the electron and the hole strongly depends on the dielectric environment. Since the latter is not uniform for carriers in a monolayer, the interaction between electron and holes deviates from the usual Coulomb potential. Excellent agreement with experiments are obtained by describing the electron-hole interaction with the Rytova-Keldysh potential[27,33]:

$$V(r) = -\frac{\pi e^2}{2r_0}\left[H_0\left(\frac{\kappa r}{r_0}\right) - Y_0\left(\frac{\kappa r}{r_0}\right)\right] \qquad (1)$$

Where e is the elementary charge, r_0 is a characteristic screening length due to the polarizability of the 2D layer, $\kappa = (\varepsilon_t + \varepsilon_b)/2$ is the average dielectric constant between the top (ε_t) and bottom (ε_b) layers, and H_0 and Y_0 are the zero-order Struve and Neumann special functions, respectively. As illustrated in Fig.3(b), a consequence of this non-Coulombic potential is that increasing the principal quantum number (and therefore the exciton radius) leads to a weaker screening, since the field lines will mostly explore the surroundings of the 2D layer, which usually has a lower dielectric constant than the TMD. The excitonic series deviates from the usual Rydberg series found in hydrogenic systems. Within this model, treating the polarizability and the reduced mass as adjustable parameters allows one to reproduce the experimentally measured energy levels of exciton states in TMDs, providing a reliable all-optical estimation of the exciton binding energy and therefore of the free particle bandgap. Recently, measurements of the exciton excited states under large out-of-plane magnetic fields have provided a direct measurement of the reduced mass, leaving the polarizability as the only adjustable parameter of the model [34–38].

Importantly, light-matter interaction is dramatically enhanced whenever the incident wave is resonance with one of the excitonic states. This has been confirmed extensively in the literature by one and two-photon absorption techniques[27,39], raman spectroscopy, up-conversion[40] and second-harmonic generation (SHG) spectroscopy[41], to cite a few examples. A recent SHG experiment perfomed on monolayer MoS_2 shows that the efficiency of the SHG process is enhanced by several orders of magnitude whenever twice the laser energy coincides with one of excitonic resonances[31]. As shown in Fig.3 (c), the SHG signal is dramatically enhanced precisely where the reflectivity spectrum indicates the presence of an excitonic absorption resonance.

2.5 Exciton spin/valley polarization and coherence

Despite having very large binding energies, excitons in TMDs belong to the Wannier-Mott class since the correlation between the electron and the hole extends over several lattice constants, as shown schematically in Fig.4(a). The exciton ground-state radius a_B is of the order of one nanometer, as recently measured in magneto-optical experiments[34,36–38]. As a consequence, the exciton wavefunction is composed of Bloch states for values of k which do not extend too far away from the K^+ and K^- valleys, as illustrated in Fig.4(b). For this reason the valley-selective optical selection rules still hold for excitons and allows one to selectively populate and detect the valley DOF of excitons with polarized lasers. However, the strong exciton binding energy results in intrinsic radiative lifetimes in the picosecond range, yielding the use of the exciton valley index for quantum information applications challenging.

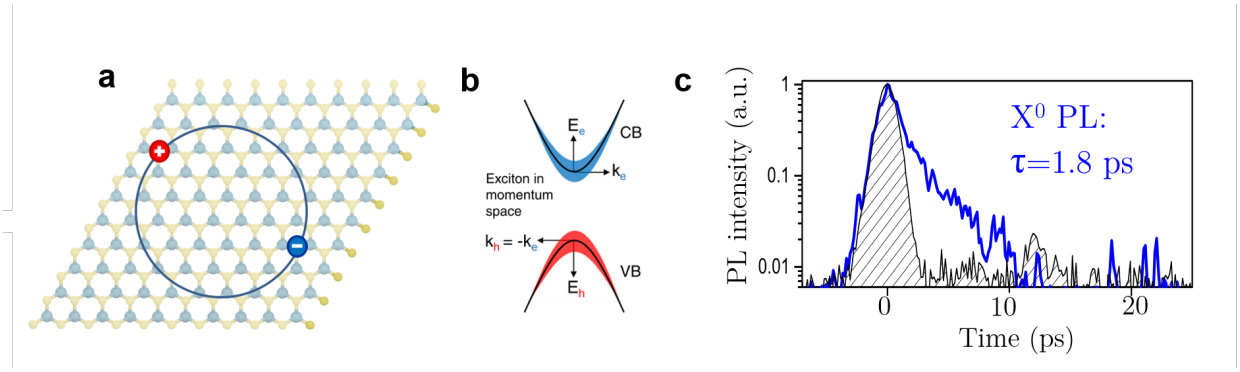

Figure 4: (a) Schematic real-space representation of the electron-hole pair bound in a Wannier-Mott exciton showing a spatial correlation spanning several elementary cells. (b) Representation of the exciton in reciprocal space with the contributions of the electron and hole quasiparticles in the conduction band (CB) and valence bands (VB), respectively, shown by the widths of the shaded areas. From [29]. (c) Time-resolved photoluminescence emission of an exciton in monolayer $MoSe_2$ at T= 4 K. Modified from [42].

For a Wannier-Mott exciton with a zero center-of-mass momentum, the radiative lifetime can be estimated by the following formula[42]:

$$\tau_{rad} = \frac{\hbar\varepsilon}{2k_0}\left(\frac{E_X}{e\hbar v}\right)^2 (a_B)^2 \qquad (2)$$

Where a_B is the exciton radius, E_X the exciton recombination energy, k_0 is the wavevector of light, $\hbar$ is Planck's constant, ε the dielectric constant and $v = \sqrt{2E_G/m_e}$ the Kane velocity with E_G the bandgap. A rough estimation yields a radiative lifetime in the ps or sub-ps range [43,44]. Experimentally, time-resolved PL experiments confirmed the short-lived nature of neutral excitons in TMD monolayers[42]. Fig.4(c) shows the measured PL of a monolayer $MoSe_2$ at cryogenic temperatures following a 150 fs laser pulse. The PL signal decays with a characteristic lifetime of around 2 ps, confirming the strong light-matter coupling of 2D excitons.

The very first optical pumping experiments on TMDs were performed on monolayer MoS_2 in 2012 [45–47]. As shown in Fig.5(a)-(b), irradiating a TMD monolayer with circularly-polarized photons generates excitons in one of the two non-equivallent K valleys. In steady-state, the resulting PL will exhibit a degree of circular polarization which reflects the competition between valley relaxation and exciton recombination. The case of ML WSe_2 following excitation with a red He-Ne laser at 4 K is shown in Fig. 5(c). The fact that the measured degree of circular polarization of the PL is smaller than 100% is an indication of the fact that valley depolarization of excitons happens in a timescale which is comparable to the recombination time, *i.e.* in the picosecond range. This valley relaxation process is around one million times faster than for resident electrons and holes, and it can be explained by Maialle-Silva-Sham (MMS) mechanism[24,48].

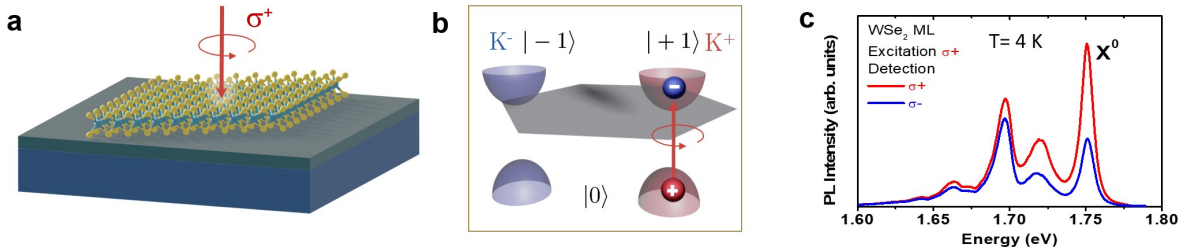

Figure 5: (a) A TMD monolayer is irradiated with a circularly-polarized laser of positive (σ^+) helicity. (b) Absorption of σ^+ photons generates excitons in the K^+ valley. (c) Polarization-resolved steady-state PL in monolayer WSe_2 at T=4 K. The circular polarization of the PL reflects the valley polarization of photoexcited excitons.

This mechanism is due to the long-range electron-hole exchange interaction. For an exciton propagating in the ML plane with a non-zero center-of-mass momentum, the eigenstates correspond to states whose dipole moment oscillates either along the wavevector (longitudinal) or perpendicular to it (transverse). These states, which are linear combinations of the states active in the σ^+ and σ^- circular polarization, are non-degenerate in energy because of the exchange interaction. The splitting between these eigenstates acts as an effective magnetic field around which the valley pseudospin precess, leading to an effective depolarization of excitons which does not need the transfer of significant momentum of a carrier nor its spin flip. As compared to excitons in traditional III-V or II-VI semiconductor quantum wells, here the longitudinal-transverse splitting is enhanced by 1 to 2 orders of magnitude due to, once again, the very strong binding between electrons and holes in TMDs.

While the very short lifetime of excitons in TMDs can be seen as an obstacle for quantum information applications, it allows on the other hand to probe coherent superpositions between the two valleys in simple PL experiments. Indeed, as the valley coherence time is comparable to the exciton lifetime at low temperatures, a coherent superposition of K^+ and K^- excitons can be maintained until the moment at which the exciton recombines.

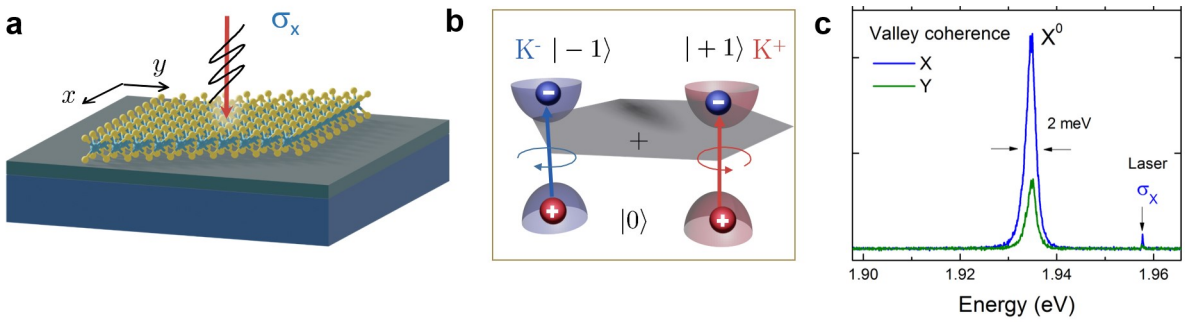

Figure 6: (a) A TMD monolayer is irradiated with a linearly-polarized laser along the x-axis. (b) Absorption of linearly-polarized photons generates a coherent superposition in which the exciton is simultaneously in both the K^+ and K^- valleys. (c) The measured steady-state PL in monolayer MoS_2 at T=4 K following a linearly-polarized excitation is partially linearly-polarized along the same direction as the incident laser. From [49].

As shown in Fig.6(a)-(b), such a coherent superposition of valley excitons can be achieved by irradiating the sample with linearly polarized light. Due to the chiral optical selection rules, each photon will be absorbed by generating an exciton in a state which is a linear superposition of K^+ and K^- states. If the phase between the two valleys in the superposition is preserved during the exciton lifetime, the PL emission will be linearly polarized along the laser's polarization axis. Experimentally, this optical generation of valley coherence in TMDs (also called exciton alignment) was first observed in 2013 in WSe_2 monolayers [20]. This valley coherence can be manipulated by the application of static out-of-plane magnetic fields, which splits in energy the two-valleys (a phenomenom known as the Valley Zeeman effect) and is responsible for a rotation of the polarization axis of the PL[49,50].

2.6 Van der Waals heterostructures and devices

While the coherent control of valley excitons has produced a revived interest in the field of valleytronics, using photo-generated excitonic species to encode spin or valley information for quantum technologies is inherently limited by both their short recombination time (~ps) [43,51,52] and their very fast spin/valley relaxation time induced by electron-hole exchange interaction (~ps) [24,48]. Thus, longer-lived excitations with stable valley/spin are required to make significant breakthroughs for quantum information applications. Among the possible candidates there are the resident carriers in doped monolayers, but they are hard to observe in PL experiments since band-to-band recombination is completely absent in the optical emission of TMDs. A recent advance in this matter was reported recently by my group and collaborators at the LPCNO (Toulouse): we have shown that the optically-induced dynamical valley polarization of resident electrons can be measured by analyzing the PL intensity of negatively-charged excitons in W-based TMDs[53]. This open the door for new fundamental studies on the valley properties of resident carriers, now with simple PL experiments.

Another promising candidate for quantum information applications is the valley/spin degree of freedom of single localized excitons at point defects, which can extend the ~1 ps

recombination lifetime of delocalized excitons up to several µs[54,55]. This is a very interesting perspective since these defects can be easily created by thermal annealing or irradiation with an electron beam[54,56]. I will discuss these localized states more in detail in the last chapter of this manuscript. Finally, new quantum quasiparticles can be engineered by the fabrication of van der Waals heterostructures.

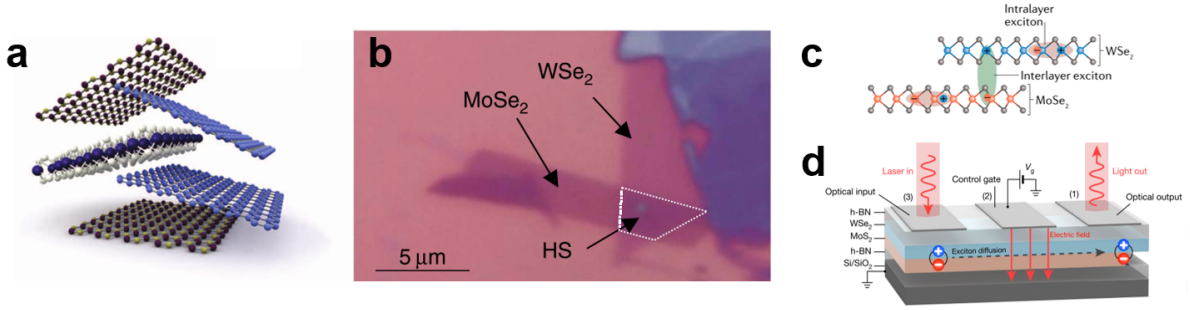

Figure 7: (a) Owing to the large variety of layered materials, van der Waals heterostructures having versatile functionalities can be fabricated by stacking different 2D materials. From [11]. (b) Optical micrograph of a $MoSe_2/WSe_2$ heterostructure (left), in which electrons are confined in one layer and holes in the other, due to the formation of a type II heterojunction in which optically injected carriers form interlayer excitons (right). From [57]. (c) Room-temperature exciton-based transistor exploiting the electric-field dependence of the interlayer exciton diffusion in a WSe_2-MoS_2 heterostructure. From[58].

Due to the weak van der Waals interactions between 2D layers, it is possible to fabricate a large variety of heterostructures by simply stacking different layered materials, in which each individual layer keeps its intrinsic properties adapted for a specific application (Fig.7(a)). A key advantage of these heterostructures with respect to their 3D counterparts is that they are expected to have lower inter-diffusion and are much less sensitive to lattice mistmatch. The first fabrication of these multi-layered devices was demonstrated for graphene and hexagonal boron nitride (hBN) – based heterostructures [59]. More recently, different hetero-bilayers of TMD of the form MoX_2/WX_2 have been fabricated. An example of such a heterostructure is shon in Fig.7(b).

The fabrication of these heterostructures allows for the control of the electronic processes and their dynamics. As mentioned above, the optical properties of TMDs are completely determinined by excitons. Fabrication of van der Waals heterostructures of the form MoX_2/WX_2 (X=S,Se) permits to strongly diminish the problem related to the fast valley relaxation of excitons, thanks to the formation of type II junctions [57,60,61]. In these systems, optically excited electron-hole pairs are separated at the interface, electrons are confined in the MoX_2 layer whereas holes in the WX_2 one, thus forming interlayer excitons (Fig.7(c)) which are less affected by the exchange interaction, and for which the valley lifetime can reach the nanosecond range[60]. The ultrafast charge transfer in type II WSe_2/MoS_2 junctions can also be used to efficiently create a population of valley-polarized holes in WSe_2 with relaxation

times of several tens of microseconds at cryogenic temperatures[61]. Moreover, the out-of-plane dipole of interlayer excitons makes them highly sensitive to out-of-plane electric fields, so that their in-plane propagation can be interrupted by the application of a gate voltage. A room-temperature transistor based on the interlayer exciton propagation was demonstrated in 2018[58]. Finally, it is nowadays common in the community to use encapsulated samples, which use flakes of hexagonal boron nitride (hBN) as protective barriers for TMD monolayers and their heterostructures. One of my main publications is related to the demonstration of a dramatic improvement on the optical quality of TMDs by hBN encapsulation[62].

2.7 The effect of disorder on the properties of 2D materials

Before 2017, most of the studies found in the literature were performed on TMD monolayers deposited (or chemically grown) onto substrates like silicon. However, the 2D nature of these semiconductors make them particularly sensitive to their environment, and silicon substrates have been shown to produce several detrimental effects on the electrical and optical properties of 2D materials which include quenching of PL and distorted crystalline structure. As shown in Fig.8(a), depositing a 2D material onto a rough substrate like silicon is responsible for a significant strain and distorsion of the lattice. In addition, 2D layers are exposed to charged impurities present on the substrate's surface and to adsorbates coming from the environment, such as hydrogen and oxygen. Already in 2016, it was shown that the substrate's roughness negatively impacts both the sharpness of the diffraction patterns and the PL yield of monolayer MoS_2 [63]. Indeed, the strain induced by the substrate can have dramatic effects on the electronic properties of TMDs, as demonstrated by scanning tunneling spectroscopy (STS) experiments performed on monolayer MoS_2 on SiO_2[64]. As shown in Fig.8(b), such monolayer exhibits both direct and indirect bandgap regions of typically 10 nm of lateral size, revealing inhomogeneous strain field on the TMD and explaining the reduction in PL yield.

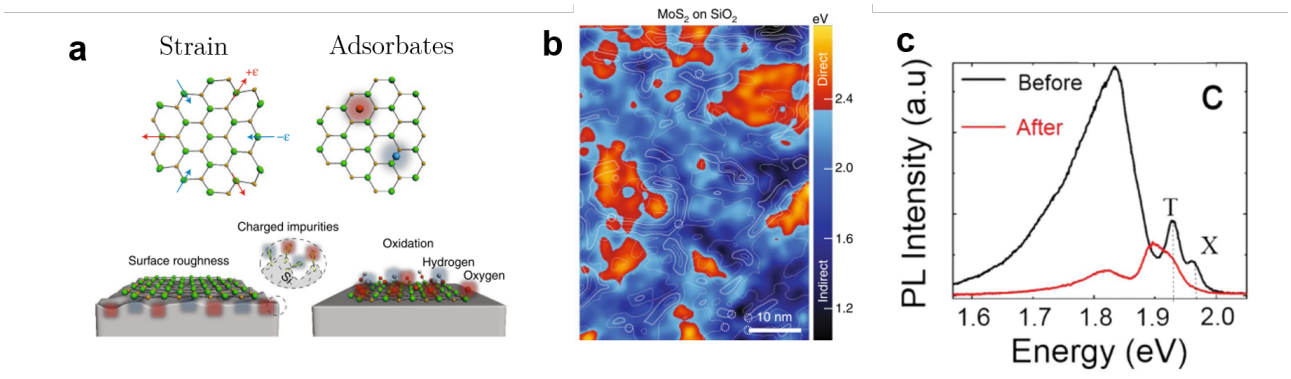

Figure 8: (a) In addition to the interaction with adsorbates like hydrogen and oxygen, 2D materials deposited onto a rough substrate like silicon are subjected to strain and charged impurities. From [65]. (b) Scanning tunnelling spectroscopy (STS) map of the bandgap in MoS_2 on an SiO_2 substrate. From [64]. (c) PL spectrum of MoS_2 on a silicon substrate at T=10 K and 0.1 µW continuous laser excitation before (black curve) and after (red curve) exposure at 24.5 µW for several minutes. From[58].

Charge puddles on the substrate are also responsible for an inhomogeneous dielectric environment, producing strong charge fluctuations in graphene [66] and inhomogeneous

broadening of the excitonic transitions in TMDs. In 2016, I have demonstrated that PL experiments on TMDs deposited onto silicon substrates were subjected to non-reversible changes due to the interaction of the laser used for photoexcitation with impurities on the silicon surface and with adsorbates on top of the monolayer. This results in a photodoping effect in which the charge density of the TMD evolves quickly after laser excitation, at laser excitation powers well below to what was considered weak by the community[67]. The PL spectrum is therefore strongly modified by the laser excitation, and the effect is most dramatic in MoS_2. As shown in Fig.8(c), the PL spectrum of monolayer MoS_2 at low temperatures strongly depends on its previous exposure to laser irradiation. After exposing the sample to a continuous laser power of 24.5 μW for a few minutes, the PL measured at a very weak photoexcitation power of 0.1 μW is completely different than for a pristine monolayer. The black spectrum (before irradiation) exhibits the neutral exciton emission as well as emission from trions and excitons bound at defects. After laser exposure, the PL spectra is that of a heavily charged monolayer, with neutral exciton emission totally quenched. This is the PL spectrum usually reported in the literature before 2016, for which the main emission peak was (wrongly) attributed to the neutral exciton emission in several works.

All these negative effects pushed the community to look for a way of protecting 2D materials from the substrate. Using thin buffer layers of hexagonal boron nitride (hBN) was shown to significantly improve the surface morphology and the electronic properties of graphene [66], reducing by more than one order of magnitude the charge fluctuations and significantly increasing the carrier mobility. For these reasons, hBN was identified as an ideal substrate for supporting 2D materials. In TMDs, the optical properties are significantly improved only after a full encapsulation with hBN, as will be discussed below.

2.8 Approaching the intrinsic homogeneous broadening by hBN encapsulation

The large Coulomb interaction in TMDs is not only responsible for large exciton binding energies but also for huge renormalization effects. As a consequence, both the free particle bandgap and the optical bandgap can be tuned, for example, by adding carriers to the system. This is typically done by applying a gate bias in contacted devices in order to add electrons or holes to the TMD monolayer. Another possibility is to engineer the dielectric environment by choosing an appropriate substrate and/or encapsulation layers. This also means that any dielectric disorder will strongly impact the properties of TMD monolayers, contributing to an inhomogeneous broadening of all the excitonic transitions. In TMDs, charge puddles present on the substrate and/or induced by adsorbates are responsible for large spatial fluctuations of both the exciton binding energy and the single-particle bandgap, as illustrated schematically in Fig.9(a)-(b). Typical PL experiments probe regions of around 1 μm of diameter, and the resulting transitions will be strongly inhomogeneously broadened. Figure 9(c) shows the typical PL spectrum of (non encapsulated) monolayer MoS_2 at low temperatures. The typical linewidth of the main transition is of 50 meV.

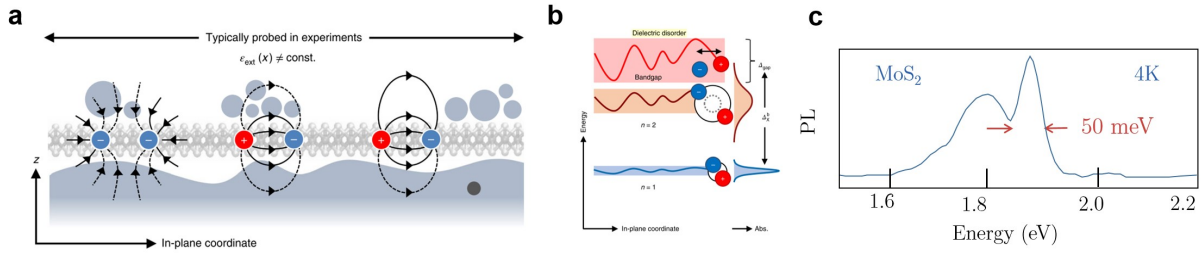

Figure 9: (a) Schematic illustration of the electron–electron and electron–hole interaction being affected by environmental screening fluctuations due to the substrate roughness, impurities and adsorbates. From [68]. (b) Illustration of the bandgap and exciton energy fluctuations due to dielectric disorder and the expected resonance broadening. From [68]. (c) PL spectrum at T=4 K of a MoS_2 monolayer, showing a linewidth of 50 meV. Modified from[69]

Although this linewidth is also due to the large photodoping effects mentioned previously, in monolayer WSe_2 and $MoSe_2$, for which photodoping effects are less dramatic, the neutral exciton transition exhibits a linewidth of typically 15 meV at low temperatures in both PL and absorption. This is still limited by inhomogeneous broadening. Indeed, for a two-level system such as the one formed by the exciton state and the crystal ground state, the homogeneous linewidth γ_h can be expressed as

$$\gamma_h = \frac{\hbar}{T_1} + \gamma^* \qquad (3)$$

where T_1 corresponds to the exciton population decay rate and γ^* is the broadening due to pure dephasing processes that destroys the phase coherence between the crystal ground state and the exciton state. Non-linear optical techniques such as four-wave mixing (FWM) are able to discriminate between homogeneous and inhomogeneous broadening. FWM measurements on TMD monolayers yield a homogeneous linewidth of the order of 1 meV at low temperatures. For example, 2 meV was reported for $MoSe_2$ at T=10 K[52], much smaller than the 15 meV PL linewidth of non encapsulated $MoSe_2$ monolayers. Note that this value permits to stablish a lower limit for the exciton lifetime of around 0.3 ps. To approach the intrinsic optical properties of TMDs, one must reduce by at least one order of magnitude the inhomogeneous broadening induced by dielectric disorder and strain. This was achieved in 2017 by a full encapsulation with hBN[49,70], which not only allows to access excitonic linewidths close to the homogeneous limit but also to get rid of non-reversible changes due to photodoping effects and substrate-induced strain. This encapsulation is now a standard procedure to access the intrinsic optoelectronic properties of layered semiconductors[71].

A schematic of such an heterostructure and an optical micrograph of a typical fabricated sample are shown in Fig.10(a) and (b), respectively. The role of hBN in these kind of heterostructures is twofold: on one hand, it is an atomically flat insulator and thus it constitutes an ideal electronic barrier so that electrons in MX_2 surrounded by hBN will stay confined in this layer. On the other hand, it avoids detrimental short range interactions with the substrate (typically SiO_2). Not only does hBN provide isolation from any surface roughness of the substrate [63], but it also acts as a barrier to charge transfer from the substrate.

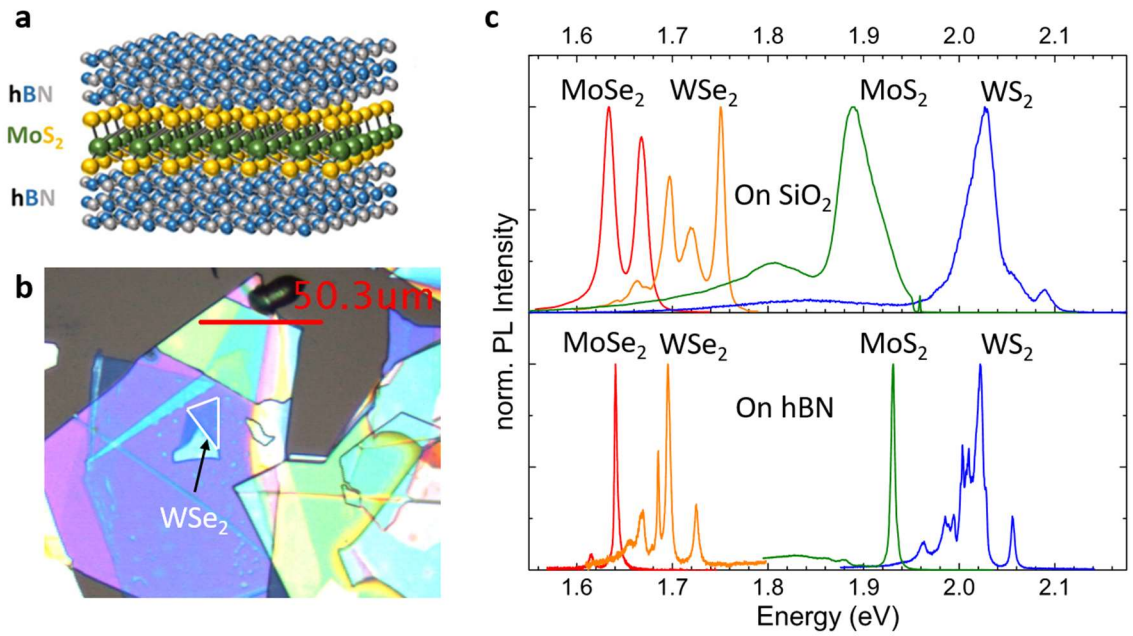

Figure 10: (a) Schematics of a hBN/MoS_2/hBN heterostructure obtained by vertical stacking of individual layers. (b) Optical micrograph of a hBN/WSe_2/hBN heterostructure. Not published yet. (c) Photoluminescence of TMD monolayers at cryogenic temperatures when deposited onto SiO2 substrates (top) and when encapsulated with hBN (bottom). From [49].

As shown in Fig.10(c), encapsulation of TMD monolayers allows for a significant improvement in the optical quality, with photoluminescence and absorption linewidths approaching the intrinsic homogeneous limit at cryogenic temperatures [62,72,73]. For MoS_2, a spectacular reduction of linewidth from 50 meV to only 2 meV is achieved after encapsulation thanks to both the reduction of dielectric disorder and the suppression of photodoping effects. Thanks to this encapsulation I have also demonstrated the optical generation of a coherent superposition of valley excitons in MoS_2 and its manipulation with static magnetic fields [62].

2.9 Selected publications

Here I present a selection of the most significant publications related to the study of 2D TMDs which highlight my research independence and the ability to supervise Ph.D. students.